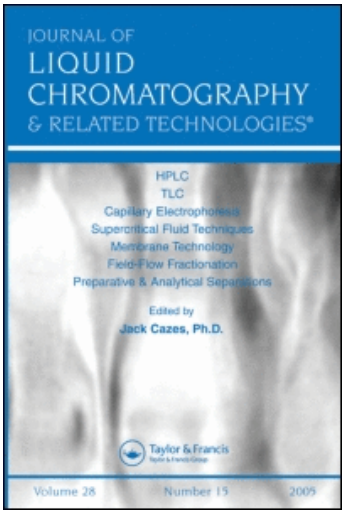

Journal of Liquid Chromatography & Related Technologies

Publication details, including instructions for authors and subscription information:
http://www.informaworld.com/smpp/title~content=t713597273

Quantitative *In Silico* Analysis of Ion Exchange from Chromatography to Protein

Toshihiko Hanai[a]
[a] Health Research Foundation Institut Pasteur, Sakyo-ku, Kyoto, Japan

To cite this Article Hanai, Toshihiko(2007) 'Quantitative *In Silico* Analysis of Ion Exchange from Chromatography to Protein', Journal of Liquid Chromatography & Related Technologies, 30: 9, 1251 — 1275
To link to this Article: DOI: 10.1080/10826070701274528
URL: http://dx.doi.org/10.1080/10826070701274528

Journal of Liquid Chromatography & Related Technologies®, 30: 1251–1275, 2007

ISSN 1082-6076 print/1520-572X online
DOI: 10.1080/10826070701274528

Quantitative *In Silico* Analysis of Ion Exchange from Chromatography to Protein

Toshihiko Hanai
Health Research Foundation Institut Pasteur, Sakyo-ku,
Kyoto, Japan

Abstract: Molecular interaction forces are based on solubility factors. Coulombic force is the strongest, followed by the Lewis acid-base interaction, including hydrogen bonding and charge-transfer effects, and van der Waals forces. Steric hindrance affects the molecular interaction. The individual interaction force can be studied using chromatography. The main interaction force in reversed-phase liquid chromatography is the van der Waals force. The main interaction force in normal phase liquid chromatography is the Lewis acid-base interaction, including hydrogen bonding, and that in ion exchange liquid chromatography is the Coulombic force. Enantiomer separation is achieved by the combination of these molecular interaction forces with steric hindrance as the molecular recognition of proteins. Previously, the retention mechanism in reversed-phase liquid chromatography was demonstrated using quantitative *in silico* analysis of chromatographic data of various compounds, such as phenolic compounds, aromatic acids, and acidic and basic drugs.[1] The retention mechanism of ion exchange liquid chromatography was then quantitatively analyzed *in silico*. Carboxyl and guanidino phases were selected for studying the basic molecular recognition mechanism of proteins, and the selective molecular recognition of D-amino acid oxidase was quantitatively analyzed *in silico*. The main molecular interaction was the Coulombic force, and the enantioselectivity was affected by the steric hindrance of the surrounding amino acid residues.

Keywords: Ion-exchange mechanism, Chromatography, Computational chemistry, Enzyme reaction

Address correspondence to Toshihiko Hanai, Health Research Foundation Institut Pasteur 5F, Tanakamonzencho, Sakyo-ku, Kyoto 606-8225, Japan. E-mail: thanai@attglobal.net

BASIC STUDY OF THE ION EXCHANGE MECHANISM

Cation Exchange

A simplified model experiment *in silico* demonstrated that carboxyl groups interact with ionized aniline by Coulombic force and with the molecular form of aniline by Lewis acid-base interaction. The specificity can be understood from the molecular interaction energy values calculated using the molecular mechanics (MM2) calculation of the CAChe program. The molecular interaction energy value (MI) is the subtracted energy value of a complex from the sum of the energy values of the pair of compounds, as given by the following Equations. The calculated energy values are summarized in Table 1.

$$\mathrm{MI(FS)} = \mathrm{FS(NH_2)} + \mathrm{FS(COO)} - \mathrm{FS(COO-NH_2\ complex)}$$
$$\mathrm{MI(HB)} = \mathrm{HB(NH_2)} + \mathrm{HB(COO)} - \mathrm{HB(COO-NH_2\ complex)}$$
$$\mathrm{MI(ES)} = \mathrm{ES(NH_2)} + \mathrm{ES(COO)} - \mathrm{ES(COO-NH_2\ complex)}$$
$$\mathrm{MI(HB)} = \mathrm{VW(NH_2)} + \mathrm{VW(COO)} - \mathrm{VW(COO-NH_2\ complex)}$$
$$\mathrm{MI(FS)} = \mathrm{FS(NH_3)} + \mathrm{FS(COO)} - \mathrm{FS(COO-NH_3\ complex)}$$
$$\mathrm{MI(HB)} = \mathrm{HB(NH_3)} + \mathrm{HB(COO)} - \mathrm{HB(COO-NH_3\ complex)}$$
$$\mathrm{MI(ES)} = \mathrm{ES(NH_3)} + \mathrm{ES(COO)} - \mathrm{ES(COO-NH_3\ complex)}$$
$$\mathrm{MI(HB)} = \mathrm{VW(NH_3)} + \mathrm{VW(COO)} - \mathrm{VW(COO-NH_3\ complex)}$$

where FS, HB, ES, and VW are the energy of the final (optimized) structure, hydrogen bonding, electrostatic, and van der Waals, respectively. NH_2 and NH_3 are the molecular and ionized forms of aniline. COO is the carboxyl phase.

The contribution of electrostatic energy was -7.937 kcal/mol, and that of hydrogen bonding was negligible because there was no hydrogen in the ionized carboxyl group in the cation exchange mode. Further studies were performed based on the difference in the atomic partial charge of the targeted atoms calculated by the PM5 model of the CAChe program. The results are shown in

Table 1. Molecular interaction (MI) values in cation exchange mode

	FS	HB	ES	VW
Molecular form aniline (NH_2)	−6.121	−1.334	0	3.416
Ionic form aniline (NH_3)	−1.048	0	0	3.496
Carboxyl group (COO)	3.370	0	0	2.954
Complex of COO-NH_2	−3.370	−1.333	−0.343	5.584
Complex of COO-NH_3	−5.691	0	−7.939	6.198
MI of COO-NH_2 complex	−1.127	0.001	−0.343	−0.786
MI of COO-NH_3 complex	−3.368	0	−7.937	−0.252

Unit: kcal/mol.

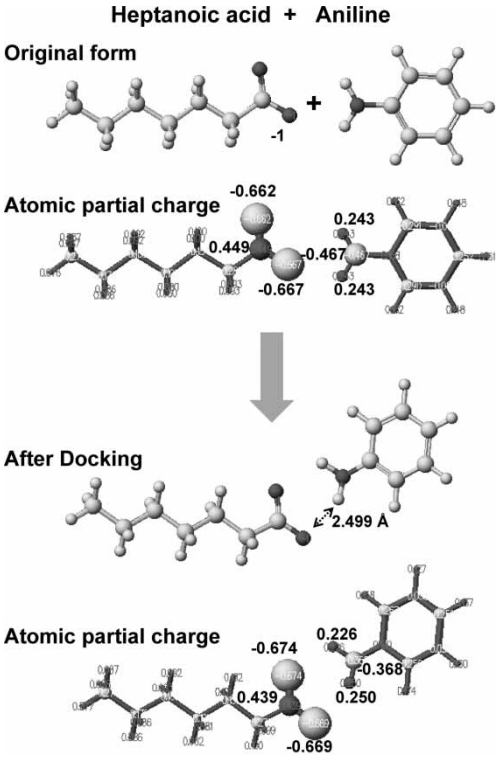

Figure 1. Molecular structure and atomic partial charge of before and after docking of aniline with ionized heptanoic acid. Small white ball: hydrogen; large white ball: carbon; gray ball: nitrogen; black ball: oxygen. Atomic partial charge, white ball: negative charge; black ball: positive charge, larger the size, higher the absolute value.

Figures 1 and 2. The atomic partial charge of the target atoms is given in the Figures, where the gray and black colors indicate negative and positive charge, respectively. The larger the size, the higher the absolute value.

The atoms of the carboxyl group of heptanoic acid and the amino group of aniline were targeted for study. The atomic partial charge of the carboxyl group oxygen was -0.662 and -0.667 in the ionized form. These values increased by approximately 0.14 after their complex formation with the ionized aniline. The values were -0.518 and -0.529, and they changed little when the complex was formed with the molecular form of aniline. The atomic partial charge of nitrogen was -0.467 in the molecular form, and that of the ionized form was 0.111. In contrast with the oxygen, the atomic partial charge of the aniline nitrogen increased by approximately 0.36 and 0.10 in the ionized and molecular forms, respectively. The atomic partial charge of one hydrogen of the ionized amino group increased significantly in the cation exchange mode. The atomic distance expanded to 1.326 Å,

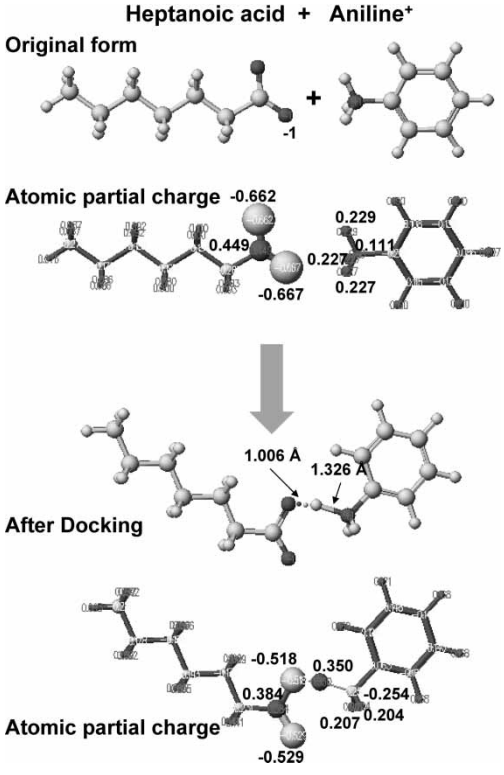

Figure 2. Molecular structure and atomic partial charge of before and after docking of ionized aniline with ionized heptanoic acid. Symbols: see Figure 1.

and the hydrogen bound weakly with the oxygen of heptanoic acid. The atomic distance was 1.006 Å. These results support the contribution of Coulombic force in cation exchange liquid chromatography.

The above findings were obtained without solvent and pH control components. The solvent and pH control components, however, contribute to the replacement of an analyte during elution from the column, and the initial molecular interaction must occur directly between the analyte and the molecular recognition phase.

Anion Exchange

The anion exchange mechanism is also understood from molecular interaction energy values calculated by the molecular mechanics (MM2) calculations of the CAChe program. The model analyte was benzoic acid and the model phase was hexyl-guanidine. The molecular interaction energy values were calculated similarly to those for cation exchange. The calculated energy values are summarized in Table 2.

Table 2. Molecular interaction (MI) values in anion exchange mode

	FS	HB	ES	VW
Molecular form benzoic acid (BAm)	−13.918	−3.459	−6.672	4.876
Ionic form benzoic acid (BAi)	−2.549	0	0	4.743
Guanidino group (GUA)	0.036	3.824	−21.680	11.376
Complex of GUA-BAm	−35.595	−8.089	−29.232	7.810
Complex of GUA-BAi	−23.514	−0.101	−27.333	8.794
MI of GUA-BAm complex	−21.714	−8.454	−0.880	−8.442
MI of GUA-BAi complex	−21.001	−3.925	−5.653	−7.325

FS, HB, ES, and VW are energy of final (optimized) structure, hydrogen bonding, electrostatic, and van der Waals, respectively. BAm and BAi are molecular and ionized form benzoic acid. GUA is guanidine phase; unit: kcal/mol.

The molecular interaction electrostatic energy value of GUA ionized benzoic acid was −5.653 kcal/mol, and that of GUA molecular form of benzoic acid was −0.880 kcal/mol. This difference clearly indicated the contribution of Coulombic force in the ion exchange system. The molecular interaction hydrogen bonding energy values of the GUA molecular form of

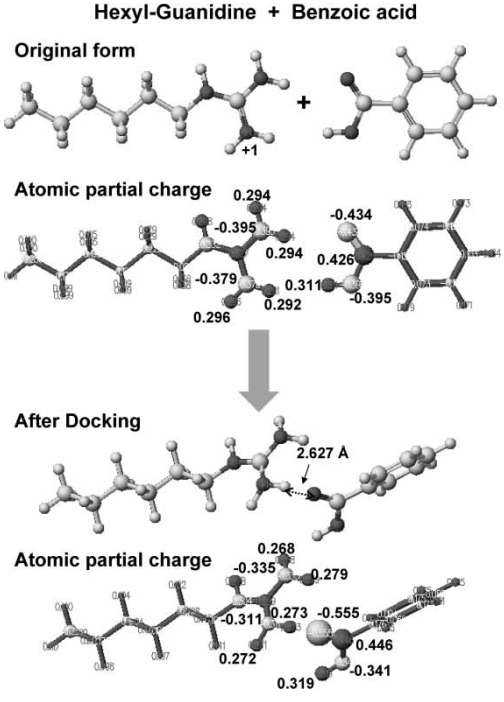

Figure 3. Molecular structure and atomic partial charge of before and after docking of benzoic acid with hexylguanidine. Symbols: see Figure 1.

benzoic acid and GUA ionized benzoic acid were −8.454 and −3.925 kcal/mol, respectively. Hydrogen bonding is not the main molecular interaction force for ionized acids, but does contribute in the ion exchange system, depending on the molecular structure of the ion exchangers. The difference can be examined based on the atomic distance and atomic partial charge of the targeted atoms. An example is shown in Figures 3 and 4. The atomic partial charge was calculated using the PM5 model of the CAChe program.

The targeted atoms were the carboxyl group of benzoic acid and the guanidino group of hexyl-guanidinine. The atomic partial charge of the carboxyl group oxygen was −0.434 and −0.395 for the molecular form, and −0.647 and −0.647 for the ionized form. These values changed after their complex formation. The values were −0.555 and −0.341 for the molecular form and −0.512 and −0.551 for the ionized form. The energy value change indicated an electron transfer in the ion exchange system. The difference is also understood from the atomic partial charge of carbon and hydrogen, as well as from the atomic partial charge change of the nitrogen and hydrogen of the guanidino group. The atomic partial charge of the hydrogen and nitrogen atoms of the guanidine group was significantly

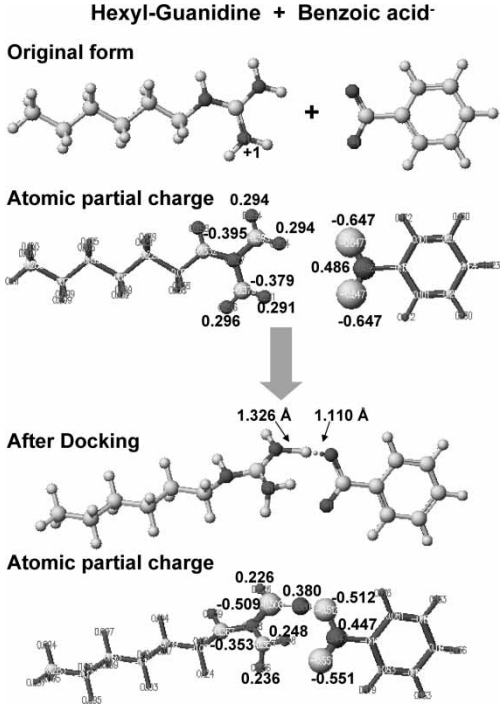

Figure 4. Molecular structure and atomic partial charge of before and after docking of ionized benzoic acid with hexylguanidine. Symbols: see Figure 1.

reduced in the ion exchange mode, compared to that of the molecular form interaction. The shortest atomic distance was 2.627 Å for the molecular form of benzoic acid. A guadinino group hydrogen weakly bonded with oxygen of the benzoic acid carbonyl group, with an atomic distance of 1.110 Å. The atomic distance between the nitrogen and the hydrogen increased from 1.005 Å to 1.326 Å. The change in atomic distance supported the strong Coulombic force in ion exchange liquid chromatography.

The above findings were obtained without solvent and pH control components. The solvent and pH control components, however, contribute to the replacement of an analyte for elution from the column, and the initial molecular interaction must occur directly between the analyte and the molecular recognition phase.

LIQUID CHROMATOGRAPHY OF BASIC DRUGS

Basic drugs were separated by cation exchange liquid chromatography using a carboxyl bonded phase. The carboxyl group mimics the cation exchange group of a protein. The retention behavior measured in liquid chromatography was quantitatively analyzed *in silico*.[2] The basic drugs used, and their molecular properties are summarized in Table 3. The computer model phase is shown in Figure 5. One carboxyl group is surrounded by alkyl groups. It looks like a little flower inside a flowerpot. The molecular interaction

Table 3. Molecular properties of basic compounds

No.	Chemicals	pKa_{ref}	pKa	MIm	MIi
1	Atropine	9.8	6.56	24.170	26.389
2	Ajmaline	8.2	5.75	32.740	33.852
3	Dextromethorphan	8.3	6.18	27.683	36.258
4	Homatropine	9.9	6.41	26.617	27.183
5	Lidocaine	7.9	5.74	24.676	30.352
6	Quinine	8.5	5.75	34.611	39.058
7	Scopolamine	7.75	4.80	26.430	27.574
8	Triamterene	6.2	3.85	24.801	30.379
9	Prazosin	6.5	4.15	28.244	25.384
10	Imipramine	9.5	6.23	27.356	39.343
11	Pyridine	5.23	3.46	14.657	17.038
12	Aniline	4.69	3.82	14.596	20.197
13	Benzylamine	9.33	6.08	16.207	22.426
14	N-Ethylaniline	9.82	6.65	17.613	23.698
15	2,4-Dimethylaniline	5.15	3.94	20.978	25.515

MIm: molecular interaction energy of molecular form; MIi: molecular interaction energy of ionized form.

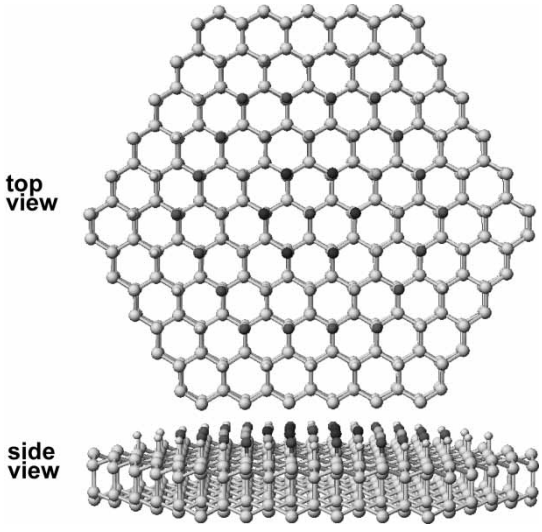

Figure 5. Basic structure of model bonded-phase.

energy values of the molecular and ionized form of the basic drugs were calculated using the molecular mechanics (MM2) function of the CAChe program.

For the development of a quantitative structure retention relationship in chromatography, the molecular interaction energy value (MI energy) was calculated between a model phase and an analyte. The optimized energy value was less than 0.00001 kcal/mol. MI energy was defined as the energy value of the complex subtracted from the sum of the energy values of the model phase and analyte

$$\mathrm{MI} = \mathrm{FS}_{\mathrm{analyte}} + \mathrm{FS}_{\mathrm{model\ phase}} - \mathrm{FS}_{\mathrm{complex}} \quad (1)$$

where FS is the energy value of the final structure (optimized structure). The MI energy values of the molecular and ionized forms of the analytes are summarized in Table 3. The MI energy values correlated with the capacity ratios measured using liquid chromatography.

Inductive Effect on p*K*a of Basic Drugs

The dissociation constant (p*K*a) of these analytes was calculated from the capacity ratios measured using eluents of pH 3.2 to 9.5. The p*K*a values obtained from the experiment were very different from those in the literature listed in Table 3. The difference was partly influenced by the methanol concentration in the eluent, but the inductive effect between the carboxyl group

of the ion exchanger and the analyte might also contribute to the difference. The relation between measured and reference values is given by the following equation:

$$\text{p}K\text{a (ion exchange LC)} = 0.612(\text{p}K\text{a reference}) + 0.538, \quad \text{r} = 0.960, \quad \text{n} = 17 \tag{2}$$

The p*K*a of aromatic acids measured using a propylamino bonded silica gel (NH_2) was smaller than that measured using an octadecyl bonded silica gel (ODS), and that measured using diethylaminoethyl bonded silica gel (DEAE) was also smaller. The p*K*a measured using a cation exchanger (SP) was shifted to a higher pH region.[3] The relations are given in the following Equations:

$$\text{p}K\text{a } (NH_2) = 0.744(\text{p}K\text{a(ODS)}) + 0.446, \text{r} = 0.988, \quad \text{n} = 29 \tag{3}$$

$$\text{p}K\text{a (DEAE)} = 0.847(\text{p}K\text{a(ODS)}) + 0.268, \text{r} = 0.990, \quad \text{n} = 29 \tag{4}$$

$$\text{p}K\text{a (SP)} = 1.023(\text{p}K\text{a(ODS)}) - 0.097, \text{r} = 0.998, \quad \text{n} = 29 \tag{5}$$

Thirty-six aromatic acids were used, but 7 aromatic acids were eliminated to determine the properties of ion exchangers. The eliminated aromatic acids demonstrated the possibility of intra-molecular hydrogen bonding.

These data were measured under the same conditions containing 20% acetonitrile. Therefore, the concentration effect of an organic modifier could be neglected for comparison. The effect of an organic modifier in the reversed phase liquid chromatography was approximately 0.022 pH unit/% of methanol or acetonitrile, experimentally.[4,5] The concentration effect of the organic modifier depended on the buffer components, even when the pH was measured using standard buffers for a pH meter with the same concentration as the organic modifier. Furthermore, the p*K*a shift in the aqueous organic solvent depended on the analyte.[6] This organic modifier effect was observed for carboxylic acid in reversed phase liquid chromatography,[7] and for polar aromatic compounds on cation exchangers and porous polymer gels.[8] The difficulty in standardizing the organic modifier effect is due to the difficulty in performing quantitative analysis of solvation. In this experiment, however, pH was measured before mixing with the organic modifier; therefore, the relatively higher pH values are a likely property of the ion exchanger used.[3]

The slope of equation (2) indicates the selectivity of the carboxyl phase. The inductive effect of the ion exchanger affects the shift of the measured p*K*a values, and the degree of the shift might depend on the ion exchange capacity, the ionic strength, and, possibly, the ionic strength of the buffer components of the eluent. The salting out effect at higher and lower pH was higher in sodium phosphate solution than that in sodium acetate solution.

Quantitative Analysis of Log *k in Silico*

Using a computational chemical calculation to analyze liquid chromatographic data, the direct interaction between a model phase and an analyte was calculated as energy values using the molecular mechanics (MM2) calculation quantitatively. For the quantitative structure retention relationship of reversed phase liquid chromatography, the contact surface area is important, and the selection of a model phase is difficult, but a simple model phase is satisfactory for the measurement of albumin acidic drug binding affinity in ion exchange liquid chromatography.[9]

The pH effect on molecular interactions can be examined experimentally using liquid chromatography. The capacity ratio in an eluent of a given pH can be predicted using the following equation:[10]

$$k = (k\mathrm{m} + k\mathrm{i}([\mathrm{H}^+]/[K])/(1 + ([\mathrm{H}^+]/[K]) \quad (6)$$

where km and ki are capacity ratios of the molecular and ionized forms of the analytes. $[\mathrm{H}^+]$ is the hydrogen ion concentration in the eluent, and $[K]$ is the dissociation constant of the analyte. The capacity ratios, km and ki, were replaced with MI energy values calculated using molecular mechanics; the km value was replaced with the MI energy value of the molecular form of the analyte (MIm) and the ki value was replaced with using the MI energy value of the ionized form of the analyte (MIi). The following Equation is used for further discussion:

$$\mathrm{MI} = (\mathrm{MIm} + \mathrm{MIi}([\mathrm{H}^+]/[K]))/(1 + ([\mathrm{H}^+]/[K])) \quad (7)$$

This led us to examine how to obtain the relative dissociation constant in ion exchange liquid chromatography. The relative pKa values measured in this cation exchange liquid chromatography were shifted to lower values compared to the reference values. The original pKa values measured by titration were affected by the organic modifier concentration and the inductive effect of ion exchange groups of the bonded phase. MI(ΔFS) was calculated using equation (7).

The model phase was based on a model phase constructed to study the ionization effect of the docking of an acidic drug with a protein.[11] The basic model structure is shown in Figure 5.

One ionized carboxyl group was located at the center of the carbon phase, and six methyl groups surrounded the carboxyl group to protect against the binding of octyl groups. There were 16 octyl groups. The longer neighbor alkyl chains were bound together by hydrophobic interactions, i.e., van der Waals energy, in this type of molecular modeling. The model phase consisted of 1350 atoms, including 2 oxygens, 739 hydrogens, 609 carbons, 1588 bonds, and 9121 connectors. An example of the complex structure is shown in Figure 6 where scopolamine was docked with the model phase.

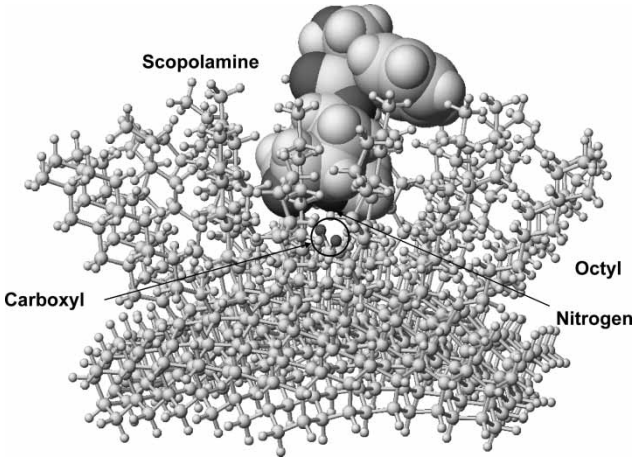

Figure 6. Docking of scopolamine with carboxyl-octyl phase; small white ball; hydrogen; large white ball: carbon; large gray ball: nitrogen; large black ball: oxygen; atom size of scopolamine is 5 times of carboxyl-octyl phase.

The correlation between MI (DFS) and the experimental log k values is given in Figure 7.

The correlation coefficient was high near the pKa values of these compounds. The correlation coefficient was poor at higher pH, where a salting out effect reduced the retention.[11]

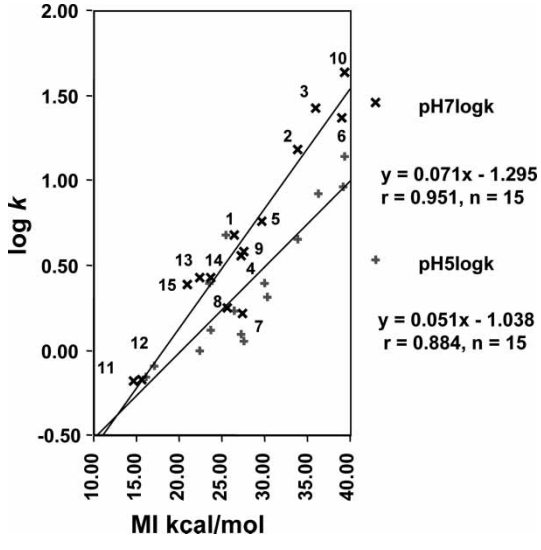

Figure 7. The correlation between MI and the experimental log k values. The numbers beside symbols see Table 3.

The molecular interaction energy values between an analyte and a model phase were determined using a direct molecular mechanics calculation using the molecular mechanics (MM2) calculation of the CAChe program, which demonstrated that retention order could be predicted, even in ion exchange liquid chromatography with a pH controlled eluent.

LIQUID CHROMATOGRAPHY OF ACIDIC DRUGS

Acidic drugs were separated in anion exchange liquid chromatography using a guanidine-bonded phase. The guanidino group mimics an anion exchange group of the protein. The chromatographic data were quantitatively analyzed *in silico*.[12] The acidic drugs used, and their molecular properties, are summarized in Table 4. The computer model of the guanidino phase is shown in Figure 8.

Inductive Effect on p*K*a for Acidic Drugs

The acidic drug p*K*a was calculated from the capacity ratios measured using eluents of pH 3.0 to 9.0. The p*K*a values obtained from the experiment were very different from those reported in the literature (see Table 4). The difference was partly influenced by the methanol concentration in the eluent, but the inductive effect between the guanidino group of the ion

Table 4. Molecular properties of acidic compounds

No.	Chemicals	pKa$_{ref}$	pKa	MIm	MIi
1	Furosemide	4.2	5.72	23.592	31.184
2	Ibuprofen	5.2	6.11	24.515	32.909
3	Indomethacin	4.5	5.83	36.477	47.386
4	Iopanoic acid	−6.05	34.23	5	39.888
5	Mefenamic acid	4.2	5.71	31.606	42.211
6	Nalidixic acid	6.0	6.43	23.849	28.415
7	Naproxen	4.2	5.71	22.827	32.190
8	Nicotinic acid	4.95	6.01	17.022	24.844
9	Phenylbutazone	4.4	5.79	28.226	42.237
10	Probenecid	3.4	5.40	24.142	37.505
11	Salicylic acid	3.0	5.24	21.661	30.691
12	Tolazamide	5.7	6.31	22.514	34.746
13	Tolbutamide	5.3	6.15	18.776	35.166
14	Warfarin	5.1	6.07	26.052	32.272

MIm: molecular interaction energy of molecular form; MIi: molecular interaction energy of ionized form.

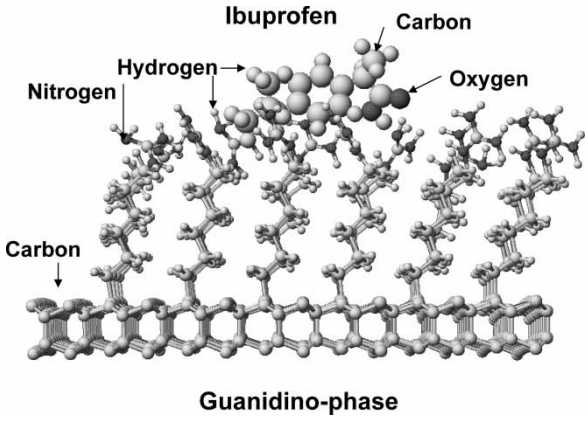

Figure 8. Docking of ibuprofen on the guanidine phase. Small white ball: hydrogen; large white ball: carbon; large gray ball: nitrogen; large black ball: oxygen; Atom size of ibuprofen is twice of the guanidino phase.

exchanger and the analyte could also contribute to the difference. The relation between the measured and reference values is given by the following equations:

$$\text{p}K\text{a (ion exchange LC)} = 0.370(\text{p}K\text{a reference}) + 4.116, \quad \text{r} = 0.792, \quad \text{n} = 13 \tag{8}$$

$$\text{p}K\text{a (ion exchange LC)} = 0.397(\text{p}K\text{a reference}) + 4.048, \quad \text{r} = 0.931, \quad \text{n} = 12 \tag{9}$$

The correlation coefficient increased from 0.792 to 0.931 after the elimination of nicotinic acid. The slopes of equations (8) and (9) indicate the selectivity of the guanidino phase. The inductive effect of the ion exchanger affects the shift of the measured p*K*a values, and the degree of the shift might depend on the ion exchange capacity and ionic strength, as well as the ionic strength of the eluent used. The salting out effect at higher and lower pH was higher for the sodium phosphate solution than for the sodium acetate solution. In the sodium acetate eluent, a strong acid (e.g., salicylic acid) was retained more than were weaker acids. The maximum retention time was not obtained with a pH 3.22 solution.

The difficulty in standardizing the effect of an organic modifier is due to the current obstacles in quantitatively analyzing solvation. In this experiment, however, pH was measured before mixing with an organic modifier. Therefore, the relatively higher p*K*a values should be a property of the ion exchanger used.[3]

Quantitative *in Silico* Analysis of Log *k*

Using computational chemical calculations to analyze liquid chromatographic data, the direct interaction between a model phase and an analyte was calculated quantitatively as energy values, using MM2 calculations. A simple model guanidino bonded phase was constructed to investigate the acidic compound guanidino phase interactions. The model phase contained 1117 atoms, 1470 bonds, and 8432 connectors, and 12 hexyl guanidino groups, and 12 hexyl groups bound on a double layer like carbon phase that maintained a rigid basic structure. The analyte was located in the center of the guanidino phase, and the complex was optimized using MM2 calculations. The optimized energy value was less than 0.00001 kcal/mol. An example of a complex form is shown in Figure 8, where ibuprofen is adsorbed on the guanidino phase.

The relative p*K*a values measured in this anion exchange liquid chromatography were shifted to higher values compared to the reference values as given in equations (8) and (9). The original p*K*a values measured by titration were affected by the organic modifier concentration and the inductive effect of the ion exchange groups of the bonded phase. Therefore, the MI at a given pH was first calculated using the measured p*K*a and equation (7). The correlation between MI and the experimental log k values is shown in Figure 9.

The contribution of intra-molecular hydrogen bonding energy was high for salicylic acid, and therefore, the final molecular interaction energy value was reduced by the original hydrogen bonding energy value of the analyte.[12]

The correlation coefficients obtained were not very high compared with those obtained for reversed phase liquid chromatography. The predicted

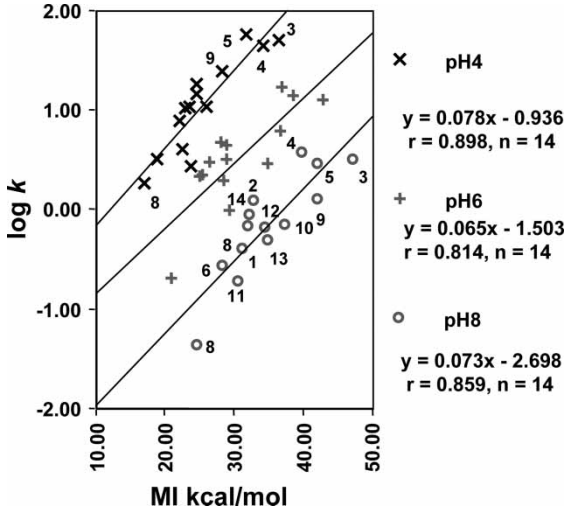

Figure 9. The correlation between MI and the experimental log *k* values. The numbers beside symbols see Table 4.

p*K*a values from the reference values measured by titration can be used if a p*K*a conversion equation, like equation (9), is obtained systematically for a specific ion exchanger. This approach is still difficult, however, due to the uncontrolled inductive effect of the ion exchange groups.

Chromatography *in silico* using a model phase was practical for studying the retention mechanism. Furthermore, elution order can be predicted even in ion exchange liquid chromatography. The difficulty is predicting the relative p*K*a values in ion exchange liquid chromatography. Compounds, however, dissociated based on their p*K*a measured by titration. Computational chemical optimization based on the molecular properties of analytes is practical in liquid chromatography, and allows for the study of molecular interactions.

MODEL STUDY OF PROTEIN-DRUG DOCKING

There are numerous reports on the three dimensional structure of proteins determined by X-ray crystallography and/or NMR, and by computational chemical calculation from the results of amino acid sequencing. An empirical approach to identifying catalytic sites, the location of metal ion and carbohydrate binding sites, and folding and unfolding, has been used with molecular dynamics simulations. A variety of different search and optimization methods have been developed for protein ligand docking applications.[13–16] Once the binding site of a protein, the structure of a protein, and a small molecule interaction are determined, the fitted small molecule is further modified, and a variety of drug candidates can be designed. One question is how a small molecule reaches the center of the protein. Agre and MacKinnon clearly demonstrated how ions and water cross cell membranes in which the existence of ion channels in a protein is important. Ions and water are driven through by electronic force. The electronic movement is Arhenius' theory of electrolytic dissociation.[17–22]

The active sites of some enzymes are nearly identical, but the catalytic reactions are different. One enzyme can have a different chemistry at the same active site. These observations indicate that a protein will bind different compounds in the same manner.[23–26] The binding mechanism should be basically the same, and it is not with 100% affinity. The basic docking mechanism can be explained by a simple model experiment.

Guanidino groups of arginine should function as anion exchange groups, and carboxyl groups of aspartic and glutamic acids should function as cation exchange groups. Determining how to design a new bonded phase to measure protein drug binding affinity using a single chromatography, is important for developing a quick screening method for drug candidates. Several model phases were constructed, and a suitable model phase was screened to demonstrate the importance of ion-ion interactions, and to explain how a small molecule reaches the center of the protein.[27]

Coulombic Force Between Guanidino and Carboxyl Groups

The model support consisted of 730 carbons, 988 hydrogens, and 11275 connectors. The center hydrogen was replaced by a methyl group or a guanidino group. The surrounding 6 hydrogens were replaced by methyl groups to make room for the analyte to contact the center substitute, and 54 hydrogens of 2nd, 3rd, and 4th circle were replaced by dodecyl groups. The bonded phase was like a tulip, and a small pocket remained where a small molecule could reach the methyl or ion exchange group at the center of the bonded phase like a bee entering the center of a tulip.

The molecular or ionized form of benzoic acid was placed outside a hole and faced toward the center methyl or guanidine group at the bottom of the pocket before starting the docking, then, the complex structure was optimized to measure the direct hydrophobic and ion ion interactions. The center substitute in the bottom of the model phase was a methyl or guanidino group. The methyl and guanidino groups represent hydrophobic and ion exchange phases, respectively. The pocket size of the phase was 8.8 Å internal diameter at the entrance, 4.4 Å at the bottom, and 12.5 Å deep. According to these pocket sizes, benzoic acid might reach the bottom without encountering a physical barrier, but a larger molecule could not reach the bottom without a strong interaction to push aside the alkyl groups.

The MI(ES) between benzoic acid and a guanidino phase demonstrated the existence of an ion ion interaction between a carboxyl ion and a guanidino group. No such energy value changes were observed for the hydrophobic phases. Even when the phenyl group was placed toward the guanidino group, a significant energy change was not obtained because benzoic acid was trapped by hydrophobic interactions before it reached the bottom of the phase. The molecular form of benzoic acid underwent hydrogen bonding with the guanidino group, but the energy change was less than that of electrostatic energy of the ionized form. A hydrogen bonding energy change was also observed on the hydrophobic phase, whose pocket size was large enough for the free access of a small molecule to reach the bottom.

Previously, furosemide was used to demonstrate the strength of Coulombic forces.[27] In the present report, further studies were performed using a larger authentic molecule shown in Figure 10. The MI energy values between the authentic molecule and GUA were obtained after a computational chemical analysis using a molecular mechanics calculation program (MM2). The optimized energy value was less than 0.00001 kcal/mol by molecular mechanics (MM2) optimization. The calculated energy values are listed in Table 5. After subtraction of the energy value of the complex from the sum of the individual energies of the analytes and a model bonded phase, the subtracted energy values were considered to be the interaction energy values (MI).

The order of MI(FS) strength is Phase-ACOO- > Phase-ACOOH > Phase-AMe. MI(ES) contributed to the strong interactions of ionized

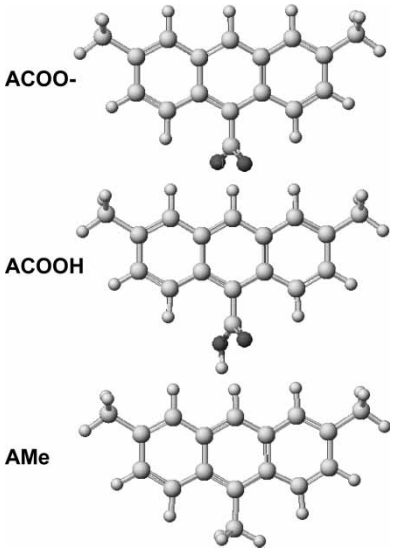

Figure 10. Structure of authentic molecule. Black ball: oxygen, large gray ball, carbon; small gray ball, hydrogen.

authentic molecules, and MI(HB) contributed to the interaction of the molecular form of authentic molecules. AMe interacted with GUA by van der Waal's force. After docking, there was little change in the atomic partial charge of authentic molecules, and the effect was as a weak as the

Table 5. Molecular properties of model phase, analytes, and molecular interaction energy values

Chemicals	FS	HB	ES	VW
ACOO-	−16.3233	0	0.004	10.626
ACOOH	−28.1879	−3.577	−6.638	10.357
AMe	−24.4248	0	0.017	11.165
Phase (GUA)	3595.2343	−0.649	−19.473	796.762
Complex of phase-ACOO	3550.4757	−0.975	−22.417	780.521
Complex of phase-ACOOH	3540.6561	−4.696	−26.514	780.678
Complex of phase-AMe	3545.7365	−0.820	−19.417	781.770
MI of phase-ACOO-	28.4353	0.326	2.948	26.867
MI of phase-ACOOH	26.3903	0.470	0.403	26.441
MI of phase-AMe	25.0730	0.171	−0.038	26.157

FS, HB, ES, VW: final structure, hydrogen bonding, electrostatic and van der Waals energy, respectively (kcal/mol); ACOO- and ACOOH: ionized and molecular form large authentic molecule; AMe: ACOOH was replaced to methyl as the blank; Phase (GUA): guanidino-phase; unit: kcal/mol.

MI(HB) of the Phase-ACOOH complex. These complex forms are shown in Figure 11A–C.

The above results demonstrated that Coulombic force (ion-ion interaction) is strong enough to drive a distance of more than 6 Å and push aside an alkyl wall whose hydrophobicity is approximately log P = 5. This means there might be a hole where a large molecule enters the protein using ion ion interactions. Further study using a real protein model is necessary.

MOLECULAR RECOGNITION OF D-AMINO ACID OXIDASE

Proteins naturally recognize enantiomers. The study of protein recognition of enantiomers was applied to analyze the reactivity of D-amino acid oxidase (DAO), which selectively oxidizes D-amino acids but not L-amino acids. This enzyme is present in a variety of organisms, such as bacteria, yeast, fungi, mollusks, insects, fish, amphibians, reptiles, birds, and mammals. Although there is only a small difference in the total number of amino acid residues, the amino acid sequences are highly conserved. The physiologic function has been reviewed.[28] The catalytic activity varies for D-amino acids. The physiologic role, stereo structure, and reaction mechanism of DAO, including its mutants, were reviewed.[29] The selective molecular recognition mechanism was studied *in silico* using the stereo structures downloaded from a protein data bank.[30]

The stereo structure of human (*Homo sapiens*) DAO was constructed based on the sequence[31] and stereo structure of pig kidney DAO,[32] where the stereo structure of human DAO was considered basically the same due to the same reaction mechanism as that of pig kidney DAO, even if the reaction selectivity was not the same. The structure is shown in Figure 12, where flavine adenine dinucleotide (FAD), and D-alanine are illustrated.

The arginine attracts D-alanine by Coulombic force like the molecular interaction between arginine and benzoic acid demonstrated in Chapter 1. The optimized energy values calculated using the MM2 calculations of the CAChe program are summarized in Table 6.

The difference in energy values of the complex with D-alanine and L-alanine is due to the optimized conformation of the initial protein conformation, as shown in Figure 12. Molecular interaction energy value favors a complex formation with D-alanine. Further study was performed using a locked structure of D- or L-alanine, FAD, and amino acid residues existed within 3 Å from the alanine, because their basic location in the protein should be maintained to analyze the ion ion interaction in the protein. The optimized conformations and atomic partial charge are shown in Figure 13A, B. The atomic distance between hydrogen and oxygen was 1.927 and 2.061 Å for the D-alanine complex, and 1.959 and 2.020 Å for

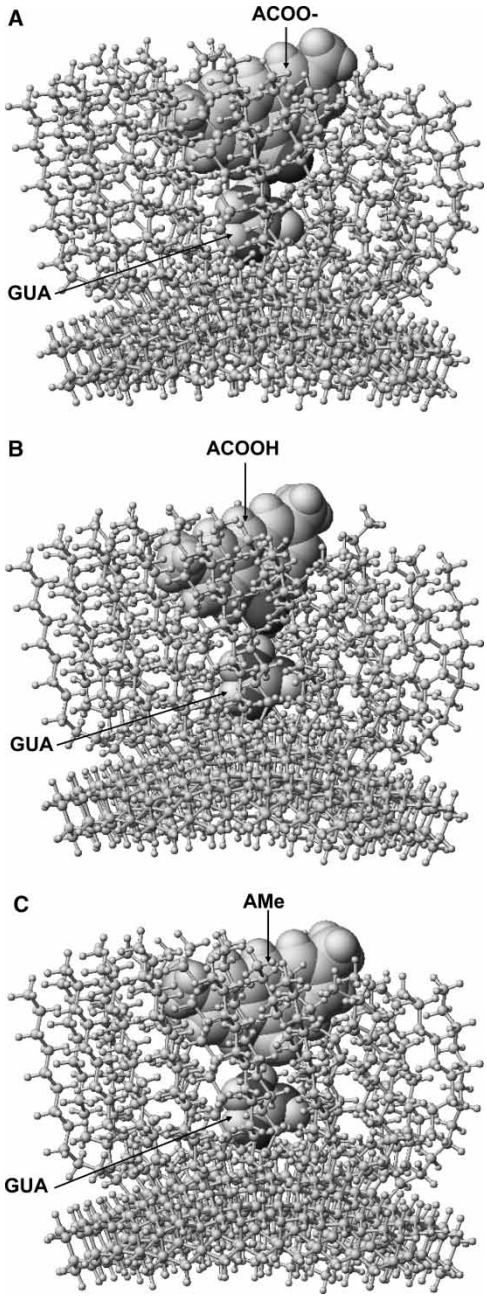

Figure 11. A–C. Structure of model phase and the complex forms. Black and dark gray ball: oxygen and nitrogen; large gray ball, carbon; small gray ball, hydrogen. Atomic size of the authentic molecule and a part of guanidine group is five times of other atoms.

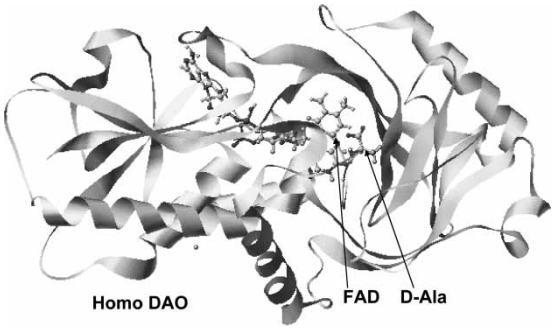

Figure 12. Optimized stereo structure of human D-amino acid oxidase (Homo DAO) and D-alanine complex.

L-alanine. Both D- and L-alanine contact the arginine guanidino group. The atomic partial charge is shown in Figure 13A and B and that of the key atoms is summarized in Table 7.

The atomic partial charge of the hydrogen in the guanidino group was a little different for D-alanine and L-alanine pairs. The small difference depends on the optimized conformation before the extraction from the protein complex. Both D- and L-alanine contacted the guanidine group, and, in this experiment, the change of atomic partial charge of the α-carbon and nitrogen of alanine favors the oxidation of D-alanine. The molecular interaction mechanism was studied using only D- or L-alanine, and a part of arginine and FAD. A part of arginine and FAD was locked and alanine was free, the complex was optimized using the MM2 calculations of the CAChe program. The conformation is shown in Figure 14. The above experiment, however, does not show such selectivity. DAO, however, selectively

Table 6. Molecular interaction (MI) energy

	FS	HB	ES	VW
Homo DAO + FAD	−6790.7798	−5147.518	−3511.330	−343.590
D-Alanine	18.9948	0	16.751	1.318
L-Alanine	19.5358	0	17.393	1.358
HomoDAO + FAD + DAla complex	−6989.0151	−5229.354	−3650.106	−340.359
Homo DAO + FAD +LAla complex	−6973.0917	−5198.819	−3651.600	−344.330
MI (DAla)	179.2405	−81.836	−155.527	−1.913
MI (LAla)	162.7761	−51.301	−157.663	2.098

FS: final (optimized) structure; HB: hydrogen bonding energy; ES: electrostatic energy; VW: van der Waals energy; FAD: flavine adenine dinucleotide; Arg: arginine; unit: kcal/mol.

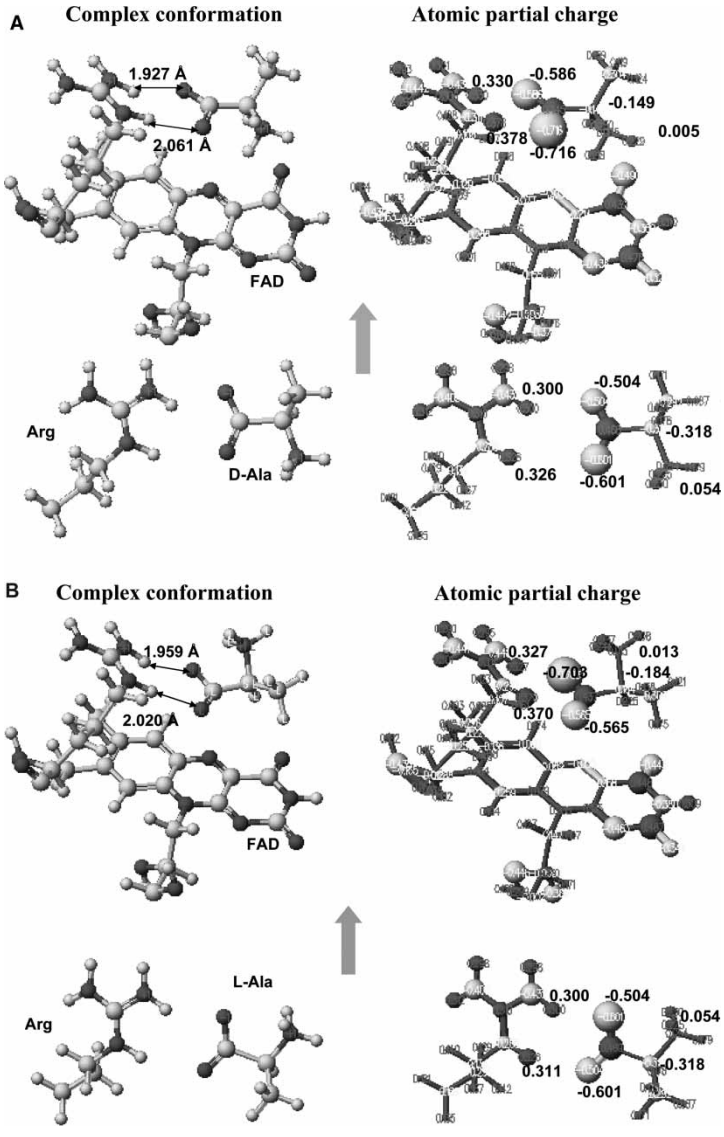

Figure 13. Complex conformation and atomic partial charge with D-alanine (A) and L-alanine (B). Small white ball: hydrogen; large white ball: carbon; gray ball: nitrogen; black ball: oxygen. Atomic partial charge, white ball: negative charge; black ball: positive charge, larger the size, higher the absolute value.

oxidizes D-amino acids, which is the stereo selectivity of the enzyme reaction. The oxidation reaction does not have any selectivity in open space, but steric hindrance of the protein results in selectivity. The conformations before removing the surrounding amino acid residues are shown in Figure 15.

Table 7. Atomic partial charge (apc) before and after docking

	Pre-docking		After docking		Δapc	
Hydrogen of guanidine group	0.300	0.326	0.330	0.378	0.030	0.052
Oxygen of D-alanine	−0.504	−0.601	−0.586	−0.716	−0.082	−0.115
Hydrogen of guanidine group	0.300	0.326	0.327	0.370	0.027	0.044
Oxygen of L-alanine	−0.601	−0.504	−0.708	−0.565	−0.102	−0.061
α-Carbon of D-alanine	−0.318	—	−0.149	—	0.165	—
α-Carbon of L-alanine	−0.318	—	−0.184	—	0.134	—
Nitrogen of D-alanine	0.054	—	0.005	—	−0.049	—
Nitrogen of L-alanine	0.054	—	0.013	—	−0.041	—

The D-alanine amino group contacts the flavine ring, but that of L-alanine is located in the opposite direction. Therefore, the oxidation reaction does not occur for L-amino acids. The DAO selectivity is not a selective molecular interaction; rather for selective reaction, L-amino acids are trapped inside of DAO and interrupt the oxidation reaction of D-amino acids.

QUANTITATIVE ANALYSIS OF THE RETENTION *IN SILICO*

The computer used was a Dell Latitude C840 equipped with a 2-GHz processor and 1024 MB memory. The molecular properties of the analytes and model phases and molecular interaction energy values were calculated using the molecular mechanics (MM2) calculations of the CAChe program (version 5; Fujitsu, Tokyo, Japan). The standard parameters used were bond stretch, bond angle, dihedral angle, improper torsion, van der Waals,

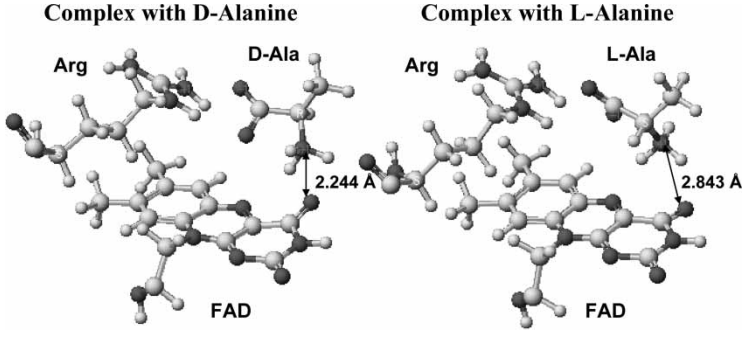

Figure 14. Complex conformation at free space. Symbols: see Figure 13.

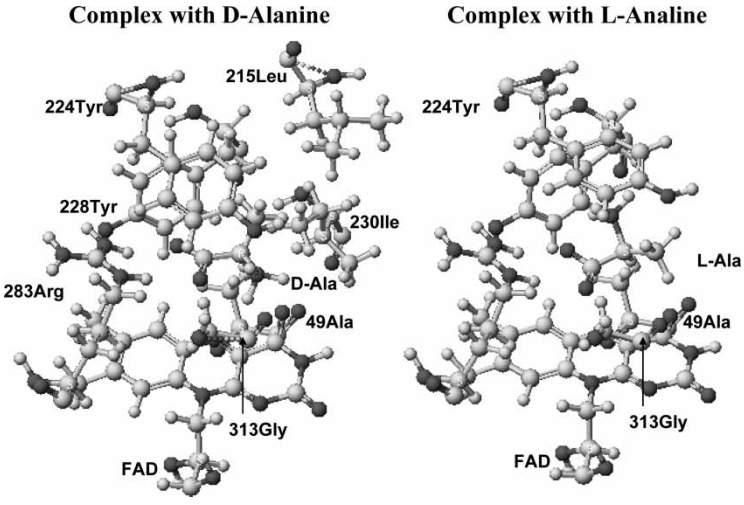

Figure 15. Conformation of D- or L-alanine complex within human D-amino acid oxidase. These structures are extracted from the original protein structures. These amino acid residues exist within 3 Å from D- or L-alanine.

hydrogen bond, and electronic forces. The van der Waals cut off distance was 9 A. The energy unit was kcal/mol (1 kJ/mol = 4.18 kcal/mol). Data analysis was performed using the Cricket-Graph program (Computer Associates, San Diego, CA) and Project Reader of the CAChe program. The molecular interaction energy values were calculated between a model phase and an analyte. The optimized energy value was less than 0.00001 kcal/mol.

A Dell Optiplex GX270 computer (Dell, Japan) was used with the CAChe computational program (version 6) for the conformational analysis of proteins. The DAO dataset (1KIF) was downloaded from the RCSB Protein Data Bank.[32] The substrate was replaced with D- or L-Ala to study the conformational change of the initial DAO. Furthermore, the stereo structure of a DAO mutant, homo sapiens DAO, was constructed based on the sequence data from NCBI[31] by substituting amino acid residues, and optimized using MM2 calculations to study the selectivity of DAO. The optimized energy value was less than 0.001 kcal/mol for proteins to reduce the calculation time.

CONCLUSION

Quantitative *in silico* of ion exchange mechanisms both in chromatography and protein was performed using model compounds. The molecular interaction energy values calculated using molecular mechanics calculations

indicated the relative strength of the molecular interactions. Particularly, the electrostatic energy value related to Coulombic force is the major contribution to ion exchange mechanisms. Further analysis using the atomic partial charge calculated by the MOPAC PM5 program clearly indicated the molecular interaction center. These approaches were applied to analyze the selective oxidation of DAO. The molecular interaction induced by Coulombic force and steric hindrance affected the reactivity.

REFERENCES

1. Hanai, T. Chromatography *in silico*, basic concept in reversed-phase liquid chromatography. Anal. Bioanal. Chem. **2005**, *382*, 708–717.
2. Hanai, T.; Masuda, Y.; Homma, H. Chromatography *in silico*; Retention of basic compounds on a carboxyl ion exchanger. J. Liq. Chromatogr. & Rel. Technol. **2005**, *28*, 3087–3097.
3. Hanai, T.; Hubert, J. Chromatography of aromatic acids on ion exchangers. J. Chromatogr. **1984**, *316*, 261–265.
4. Hanai, T.; Hubert, J. Chromatographic behavior of acids on macro porous-polystyrene gels. Chromatographia **1983**, *17*, 633–639.
5. Hanai, T.; Tran, K.C.; Hubert, J. Prediction of retention times for aromatic acids in liquid chromatography. J. Chromatogr. **1982**, *239*, 385–394.
6. Roses, M.; Bosch, E. Influence of mobile phase acid-base equilibria on the chromatographic behavior of protolytic compounds. J. Chromatogr. A **2002**, *982*, 1–30.
7. Van de Venne, J.L.M.; Hendrikx, J.L.H.M.; Deelder, R.S. Retention behavior of carboxylic acids in reversed-phase column liquid chromatography. J. Chromatogr. **1978**, *167*, 1–16.
8. Hanai, T.; Walton, H.F.; Navratil, J.D.; Warren, D. Liquid chromatography of polar aromatic compounds on cation exchange resins and porous polymer gels. J. Chromatogr. **1978**, *155*, 261–271.
9. Hanai, T.; Miyazaki, R.; Kamijima, E.; Homma, H.; Kinoshita, T. Computational prediction of drug-albumin binding affinity by modeling liquid chromatography interactions. Internet Electr. J. Molec. Des. **2003**, *2*, 702–711.
10. Pietrzyk, D.J.; Chu, C.-H. Separation of organic acids on Amberlite XAD copolymers by reversed-phase high pressure liquid chromatography. Anal. Chem. **1977**, *49*, 860–867.
11. Hanai, T. Molecular modeling for quantitative analysis of molecular interaction. Lett. Drug Disc. Des. **2005**, *2*, 232–238.
12. Hanai, T.; Homma, H. Chromatography *in silico*, Retention of acidic drugs on a guanidine ion exchanger. J. Liq. Chromatogr. & Rel. Technol. In press.
13. Mancera, R.L.; Kallblad, P.; Todorov, N.P. Ligand-protein docking using a quantum stochastic tunneling optimization method. J. Comput. Chem. **2004**, *25*, 858–864.
14. Tatsumi, R.; Fukunishi, Y.; Nakamura, H. A hybrid method of molecular dynamics and harmonie dynamics for docking of flexible ligand to flexible receptor. J. Comput. Chem. **2004**, *25*, 1995–2005.
15. Kallblad, P.; Mancera, R.L.; Todorov, N.P. Assessment of multiple binding modes in ligand-protein docking. J. Med. Chem. **2004**, *47*, 3334–3337.

16. Kontoyianni, M.; McClellan, L.M.; Sokol, G.S. Evaluation of docking performance: comparative data on docking algorithms. J. Med. Chem. **2004**, *47*, 558–565.
17. Preston, G.M.; Carroll, T.P.; Guggino, W.B.; Agre, P. Appearance of water channels in Xenopus oocytes expressing red cell CHIP28 protein. Science **1992**, *256*, 385–387.
18. Walz, T.; Hirai, T.; Murata, K.; Heymann, J.B.; Mitusoka, K.; Fujiyoshi, Y.; Smith, B.L.; Agre, P.; Engel, A. The three-demensional structure of aquaporin-1. Nature **1997**, *387*, 624–627.
19. Doyle, D.A.; Morais Cabral, J.; Pfuetzner, P.A.; Kuo, A.; Gulbis, J.M.; Cohen, S.L.; Chait, B.T.; MacKinnon, R. The structure of the potassium channel: molecular basis of K^+ conduction and selectivity. Science **1998**, *280*, 69–77.
20. Fu, D.; Libson, A.; Miercke, L.J.; Weitzman, C.; Nollert, P.; Krucinski, R.M. Structure of a glycerol-conducting channel and the basis for its selectivity J. Stroud R.M. Science **2000**, *290*, 481–486.
21. Sui, H.; Han, B.-G.; Lee, J.K.; Walian, P.; Jap, B.K. Structural basis of water-specific transport through the AQP-1 water channel. Nature **2001**, *414*, 872–878.
22. Yarnell, A. Renaissance men. Chemistry nobelists solved basic problems about how ions and water cross cell membranes. C&EN **2003**, *81* (November 3), 35–38.
23. James, L.C.; Tawfik, D.S. Catalytic and binding poly-reactivities shared by two unrelated proteins: the potential roll of promiscuity in enzyme evolution. Protein Sci. **2001**, *10*, 2600–2607.
24. Seffernick, J.L.; Wackett, L.P. Rapid evolution of bacterial catabolic enzymes: a case study with atrazine chlorohydrolase. Biochemistry **2001**, *40*, 12747–53.
25. Schmidt, D.M.Z.; Mundorff, E.C.; Dojka, M.; Bermudez, E.; Ness, J.E.; Govindarajan, S.; Babbitt, P.C.; Minshull, J.; Gerlt, J.A. Evolutionary potential of (B/A)8-barrels; Functional promiscuity produced by single substituents in the enalase superfamily. Biochemistry **2003**, *42*, 8387–8793.
26. Yarnell, A. The power of promiscuity. C&E News **2003**, *81* (December 8), 33–35.
27. Hanai, T. Molecular modeling for quantitative analysis of molecular interaction. Lett. Drug Des. Disc. **2005**, *2*, 232–238.
28. Konno, R.; Yasumura, Y. D-Amino acid oxidase and its physiological function. Int. J. Biochem. **1992**, *24*, 519–524.
29. Pilone, M.S. D-Amino acid oxidase: new finding. Cell Mol. Life Sci. **2000**, *57*, 1732–1747.
30. Hanai, T. Quantitative *in silico* analysis of molecular recognition and reactivity of D-amino acid oxidase. Internet Elect. J. Mol. Des. **2006**, *5*, 247–259.
31. NP 001908, D-amino acid oxidase [HOMO SAPIENS], www.ncbi.nlm.gov/entrez/query.fcgi.
32. RCSB Protein Data Bank, www.rcsb.org/pdb/.

Received January 8, 2007
Accepted January 31, 2007
Manuscript 6024